Antenna Bandwidth Optimization with Single Frequency Simulation

Cismasu, Marius; Gustafsson, Mats

2013

CODEN:LUTEDX/(TEAT-7227)/1-19/(2013)
Revision No. 1: February 2014

Antenna Bandwidth Optimization with Single Frequency Simulation

Marius Cismasu and Mats Gustafsson

Electromagnetic Theory
Department of Electrical and Information Technology
Lund University
Sweden

Marius Cismasu
Marius.Cismasu@eit.lth.se

Department of Electrical and Information Technology
Electromagnetic Theory
Lund University
P.O. Box 118
SE-221 00 Lund
Sweden

Mats Gustafsson
Mats.Gustafsson@eit.lth.se

Department of Electrical and Information Technology
Electromagnetic Theory
Lund University
P.O. Box 118
SE-221 00 Lund
Sweden

Editor: Gerhard Kristensson

Abstract

A method to compute antenna Q using an electromagnetic simulation at a single frequency is described. This method can easily be integrated into global optimization algorithms. In this way the optimization time of some antenna parameters, *e.g.*, bandwidth, may be significantly reduced. The method is validated by direct comparison with the physical bound of the analyzed structure. Numerical examples for rectangular antennas and antennas with a rectangular ground plane illustrate the integration of the method into a genetic algorithm. The results predicted by optimization agree very well with those obtained using a commercial electromagnetic solver. These results suggest that the method can be used to yield antennas with Q factors within 20 % of their corresponding physical bound.

1 Introduction

Antenna performance may be improved, when necessary, through global optimization algorithms. Mathematical considerations and examples of such algorithms are presented in [3, 5, 17]. Deterministic approaches are prohibitive for some antenna optimization problems due to the size and unpredictability of the solution space studied. However, heuristic methods, *e.g.*, genetic algorithms, particle swarm optimization, etc., have provided reasonable solutions to such problems [13, 16, 21–23]. One parameter frequently included in antenna optimization goals is the bandwidth. This parameter is commonly evaluated from multiple frequency samples of the antenna input impedance. The computation of these samples accounts in general for the greatest part of the solution time of an optimization algorithm.

Here, we estimate the Q factor from the current excited on an antenna computed at a single frequency. Using the results by Vandenbosch [24] and Geyi [4] we compute the electric and magnetic energies stored in the fields excited by an antenna and the radiated power. We assume the studied antennas are electrically small, *i.e.*, $Q \gg 1$, such that the error in the Q computation is negligible (equal to $ka \ll 1$ [11]). The previously introduced computation is performed following the procedure in [8, 10], at a single frequency, usually the center of the intended operating band. Considering the input impedance of antennas described by a resonance model [7, 26], the Q factor can be used as a direct measure of the bandwidth. This approach for computing the Q factor is implemented in a standard Method of Moments (MoM) code [8, 10]. The implementation requires minor modifications of the code and does not increase the computation time significantly.

This method is applied to antennas that may take arbitrary shapes within a rectangular region. A genetic algorithm (GA) with MoM simulation is implemented following the GA/MoM approach described in [16, 21, 23]. Using rectangular mesh elements, a mother impedance matrix is computed prior to launching the actual optimization. Similar "mother" matrices are computed at the same time for the stored electric and magnetic energies and radiated power. This approach reduces the actual optimization process to finding the rows and columns of these mother matrices that give optimum performance. A more realistic situation is also considered that

describes typical devices with limited space for antennas. Such situations resulting in large solution times can be more efficiently handled by imposing a block matrix decomposition as described in [16, 21]. The results are verified using the commercial electromagnetic solver Efield[1]. The agreement between the Q factors resulting from optimization and simulation is very good.

Antenna performance is evaluated during optimization as a linear combination of three parameters. These parameters are the Q-factor, the difference between the stored electric and magnetic energies, and metallic area (all appropriately normalized). They have been chosen to illustrate the single frequency antenna Q computation method. Other important parameters such as losses, radiation resistance or matching are not considered here. The energy-difference mentioned above represents the quantitative measure of self-resonance used during optimization. This resonance was compared with the corresponding resonance of the input impedance obtained from the commercial solver Efield. The optimization-predicted and impedance self-resonance agree to a large extent, confirming the validity of the expressions in [4, 10, 11, 24].

Physical bounds can be used to evaluate the optimization solution quality and stop an optimization process. The performance of the structures considered here has been compared with the physical bounds for rectangular structures [6, 9, 10], and structures with a rectangular ground plane [8]. This comparison shows that the optimized structures perform close to their physical bounds. In addition the rectangular ground plane results verify the theory presented in [8].

The paper is organized as follows. The method to compute the Q factor of antennas using a single frequency electromagnetic solution obtained from an MoM solver is described in Sec. 2. A possible integration of this method in a genetic rectangular antenna optimization algorithm is presented in Sec. 3.1. Further improvements to this algorithm for fixed pattern antennas are described in Sec. 3.2. The physical bounds used to compare the optimized antenna performance are described in Sec. 4. Section 5.1 describes the setup for the numerical simulations performed. Sections 5.2 and 5.3 present numerical results for rectangular antennas and antennas with a rectangular ground plane respectively. The paper ends with conclusions in Sec. 6.

2 Computation of Antenna Q in the Method of Moments

The quality factor of a lossless antenna is defined as [26]

$$Q = \frac{2\mathrm{c}_0 k \max\{W_\mathrm{e}, W_\mathrm{m}\}}{P_\mathrm{rad}}, \tag{2.1}$$

where c_0 is the speed of light in free space, k is the wavenumber, W_e and W_m are respectively the electric and magnetic energies stored in the fields excited by the

[1] www.efieldsolutions.com

antenna, and P_{rad} is the power radiated by the antenna. This definition is valid both for resonant and non-resonant antennas. Equation (2.1) is equivalent to the definition in [1] for resonant antennas.

A resonance model can be used to describe many antennas, [7, 26]. This model allows an approximation that relates the input impedance behavior to the Q factor of antennas:

$$Q_{\mathrm{Z}'} = \frac{k_0 |Z'(k_0)|}{2R(k_0)}, \tag{2.2}$$

where k_0 is the resonance wavenumber, Z' is the first derivative with respect to the wavenumber of the input impedance (tuned to resonance), and R is the radiation resistance. Equation (2.2) requires the input impedance be known at least for two different frequencies. This multiple frequency requirement is not necessary for evaluating (2.1). In this case it suffices to know the stored energies and radiated power at a single frequency. From these single frequency quantities the bandwidth can be estimated based on its inverse proportionality to the Q factor [26].

The stored electric and magnetic energies in (2.1) can be expressed using the results in [4, 24]. Here we consider, for simplicity, surface currents. The stored electric and magnetic energies are respectively $W_{\mathrm{e}} = \mu_0 w^{(\mathrm{e})}/(16\pi k^2)$ and $W_{\mathrm{m}} = \mu_0 w^{(\mathrm{m})}/(16\pi k^2)$, see also [11]. Correspondingly the total radiated power is $P_{\mathrm{rad}} = \eta_0 p^{(\mathrm{rad})}/(8\pi k)$. In the previous expressions μ_0 and η_0 are respectively the free space permeability and impedance, and

$$w^{(\mathrm{e})} = \int_{\partial V}\int_{\partial V} \nabla_1 \cdot \boldsymbol{J}_1 \nabla_2 \cdot \boldsymbol{J}_2^* \frac{\cos(kR_{12})}{R_{12}} - \frac{k}{2}\big(k^2 \boldsymbol{J}_1 \cdot \boldsymbol{J}_2^* - \nabla_1 \cdot \boldsymbol{J}_1 \nabla_2 \cdot \boldsymbol{J}_2^*\big) \sin(kR_{12})\, \mathrm{dS}_1\, \mathrm{dS}_2, \tag{2.3}$$

$$w^{(\mathrm{m})} = \int_{\partial V}\int_{\partial V} k^2 \boldsymbol{J}_1 \cdot \boldsymbol{J}_2^* \frac{\cos(kR_{12})}{R_{12}} - \frac{k}{2}\big(k^2 \boldsymbol{J}_1 \cdot \boldsymbol{J}_2^* - \nabla_1 \cdot \boldsymbol{J}_1 \nabla_2 \cdot \boldsymbol{J}_2^*\big) \sin(kR_{12})\, \mathrm{dS}_1\, \mathrm{dS}_2, \tag{2.4}$$

and

$$p^{(\mathrm{rad})} = \int_{\partial V}\int_{\partial V} \big(k^2 \boldsymbol{J}_1 \cdot \boldsymbol{J}_2^* - \nabla_1 \cdot \boldsymbol{J}_1 \nabla_2 \cdot \boldsymbol{J}_2^*\big) \frac{\sin(kR_{12})}{R_{12}}\, \mathrm{dS}_1\, \mathrm{dS}_2, \tag{2.5}$$

where $\boldsymbol{J}_1 = \boldsymbol{J}(\boldsymbol{r}_1)$, $\boldsymbol{J}_2 = \boldsymbol{J}(\boldsymbol{r}_2)$ and $R_{12} = |\boldsymbol{r}_1 - \boldsymbol{r}_2|$ are short notations for the surface current density $\boldsymbol{J}$ flowing on the boundary of volume V occupied by the entire structure and position vector $\boldsymbol{r}$.

The computation of stored energies and radiated power using (2.3), (2.4), and (2.5) is straight forward if implemented as an extension of an MoM code. Usual MoM solutions of the electric field integral equation (EFIE) use a set of local basis functions to approximate the surface current excited on the analyzed structure by a certain source [19]. Denoting by $\boldsymbol{\psi}_p$ the basis functions, this approximation is

$$\boldsymbol{J}(\boldsymbol{r}) \approx \sum_{p=1}^{N} J_p \boldsymbol{\psi}_p(\boldsymbol{r}). \tag{2.6}$$

The unknowns of the algorithm with this discretization are the coefficients $\mathbf{J} = (J_1, J_2, \ldots, J_N)^{\mathrm{T}}$. These coefficients are determined from the system of equations $\mathbf{ZJ} = \mathbf{V}$ where $\mathbf{V}$ is a discrete representation of the incident field (*e.g.*, the voltage gap model) and $\mathbf{Z}$ is the normalized impedance matrix computed based on a mixed potential formulation (equivalent to EFIE [15]) with the elements [19], normalized to $\eta_0/(4\pi k)$,

$$Z_{pq} = \mathrm{j}\int_{\partial V}\int_{\partial V}\left(k^2\boldsymbol{\psi}_p(\boldsymbol{r}_1)\cdot\boldsymbol{\psi}_q(\boldsymbol{r}_2) - \nabla_1\cdot\boldsymbol{\psi}_p(\boldsymbol{r}_1)\nabla_2\cdot\boldsymbol{\psi}_q(\boldsymbol{r}_2)\right)\frac{\mathrm{e}^{-\mathrm{j}kR_{12}}}{R_{12}}\,\mathrm{dS}_1\,\mathrm{dS}_2. \quad (2.7)$$

With the discretization defined by (2.6) the stored electric energy can be approximated using

$$w^{(\mathrm{e})} \approx \sum_{p=1}^{N}\sum_{q=1}^{N} J_p^* X_{\mathrm{e},pq} J_q = \mathbf{J}^{\mathrm{H}}\mathbf{X}_{\mathrm{e}}\mathbf{J}. \quad (2.8)$$

Apart from $\mathbf{X}_{\mathrm{e}}$, two other matrices, $\mathbf{X}_{\mathrm{m}}$ and $\mathbf{R}_{\mathrm{rad}}$, are introduced in a similar way respectively for the approximation of the stored magnetic energy and radiated power. These matrices have the same dimension as the impedance matrix, $N \times N$, and the elements:

$$X_{\mathrm{e},pq} = \int_{\partial V}\int_{\partial V}\nabla_1\cdot\boldsymbol{\psi}_{p1}\nabla_2\cdot\boldsymbol{\psi}_{q2}\frac{\cos(kR_{12})}{R_{12}} - \frac{k}{2}\left(k^2\boldsymbol{\psi}_{p1}\cdot\boldsymbol{\psi}_{q2} - \nabla_1\cdot\boldsymbol{\psi}_{p1}\nabla_2\cdot\boldsymbol{\psi}_{q2}\right)\sin(kR_{12})\,\mathrm{dS}_1\,\mathrm{dS}_2, \quad (2.9)$$

$$X_{\mathrm{m},pq} = \int_{\partial V}\int_{\partial V}k^2\boldsymbol{\psi}_{p1}\cdot\boldsymbol{\psi}_{q2}\frac{\cos(kR_{12})}{R_{12}} - \frac{k}{2}\left(k^2\boldsymbol{\psi}_{p1}\cdot\boldsymbol{\psi}_{q2} - \nabla_1\cdot\boldsymbol{\psi}_{p1}\nabla_2\cdot\boldsymbol{\psi}_{q2}\right)\sin(kR_{12})\,\mathrm{dS}_1\,\mathrm{dS}_2, \quad (2.10)$$

and

$$R_{\mathrm{rad},pq} = \int_{\partial V}\int_{\partial V}\left(k^2\boldsymbol{\psi}_{p1}\cdot\boldsymbol{\psi}_{q2} - \nabla_1\cdot\boldsymbol{\psi}_{p1}\nabla_2\cdot\boldsymbol{\psi}_{q2}\right)\frac{\sin(kR_{12})}{R_{12}}\,\mathrm{dS}_1\,\mathrm{dS}_2. \quad (2.11)$$

With these notations the Q factor (2.1) becomes

$$Q \approx \frac{\max\{\mathbf{J}^{\mathrm{H}}\mathbf{X}_{\mathrm{e}}\mathbf{J}, \mathbf{J}^{\mathrm{H}}\mathbf{X}_{\mathrm{m}}\mathbf{J}\}}{\mathbf{J}^{\mathrm{H}}\mathbf{R}_{\mathrm{rad}}\mathbf{J}}. \quad (2.12)$$

Quadratic forms similar to $\mathbf{J}^{\mathrm{H}}\mathbf{R}_{\mathrm{rad}}\mathbf{J}$ have been used in [14, 20] to express different types of power in radiating structures printed on dielectric substrates. These expressions have been further employed in the optimization of the radiation efficiency. A similar approach has been followed in the optimization of antenna arrays in free space [12].

As stated in the previous paragraph, an MoM solver can be extended to compute (2.9), (2.10) and (2.11). This extension does not significantly increase the

computational complexity of the solver. We compare the original impedance matrix $\mathbf{Z}$ with the newly introduced matrices $\mathbf{X}_\mathrm{e}$, $\mathbf{X}_\mathrm{m}$ and $\mathbf{R}_\mathrm{rad}$. This comparison shows that

$$Z_{pq} = R_{\mathrm{rad},pq} + \mathrm{j}(X_{\mathrm{m},pq} - X_{\mathrm{e},pq}), \tag{2.13}$$

and the second and third terms of $X_{\mathrm{e},pq}$ and $X_{\mathrm{m},pq}$ (correction terms introduced in [24]) are both equal to

$$-\frac{k}{2}\int_{\partial V}\int_{\partial V}\left(k^2\boldsymbol{\psi}_{p1}\cdot\boldsymbol{\psi}_{q2} - \nabla_1\cdot\boldsymbol{\psi}_{p1}\nabla_2\cdot\boldsymbol{\psi}_{q2}\right)\sin(kR_{12})\,\mathrm{dS}_1\,\mathrm{dS}_2. \tag{2.14}$$

Equation (2.13) gives the elements of $\mathbf{R}_\mathrm{rad}$ directly. The same equation gives the first terms of $X_{\mathrm{m},pq}$ and $X_{\mathrm{e},pq}$. Little computational effort is required to separate these terms from the imaginary part of Z_{pq}. The remaining correction terms (2.14) are non-singular. Their computation can be integrated in the calculation of the impedance matrix (2.7). These correction terms resemble the imaginary part of Z_{pq} except for the term causing the singularity, R_{12}. This resemblance can be utilized to reduce the computational overhead required by the correction term calculation with a standard MoM code.

In addition to the Q factor computation, the relationship between the energies stored in the fields can be used as a measure of resonance. These energies are equal when the antenna is self resonant.

3 Implementation Example

3.1 Rectangular Regions

Infinitely thin lossless, *i.e.*, perfectly electrically conducting (PEC), metallic structures are considered in the following. These structures may take arbitrary shapes within a rectangular region with the length l and width h. In order to limit the arbitrariness to a finite set of possible solutions, a discretization rule is established following the approach in [8, 10]. The natural choice is to use the same discretization as in the MoM solver used to determine the electromagnetic solution. This simplifies the optimization procedure and the MoM algorithm, as described in the following. Even though triangular mesh elements are more common, rectangular mesh elements [12, 18] pertain better to the considered regular shapes and illustration purposes of this study. Using rectangular mesh element discretization the optimal structures may take arbitrary shapes made of any of the mesh elements within the rectangular region. An example of such an antenna is depicted in Fig. 1.

The solution space of the optimization problem is made of all possible combinations of discrete elements. There are $2^{N_xN_y}$ such combinations, where N_x and N_y are the number of mesh elements in the x and y directions, respectively. Usually the number of combinations is large rendering prohibitive to study all solutions in the solution space.

One class of algorithms that search through an unknown solution space are heuristic global optimizers, *e.g.*, genetic algorithms, random search, particle swarm,

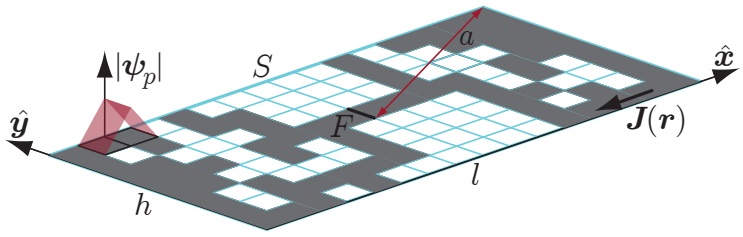

Figure 1: Example of discrete arbitrary structure within a rectangular region. The uniform rectangular grid defines the discretization of the region. Gray-shaded elements represent metallic patches on which a surface current density $\boldsymbol{J}(\boldsymbol{r})$ can exist. The feeding edge is marked F. The "rooftop" amplitude of one of the basis functions is represented in transparent red shading.

ant colony, etc. Genetic algorithms have been used in electromagnetic optimization with remarkable results, see [13, 21, 23] for a description of the method and its applications. It is known that genetic algorithms feature an acceptably fast convergence to suboptimal solutions and avoid local extrema [21]. A genetic algorithm has been chosen here due to its well known principles, ease of adjustment and availability of sample codes. Other global optimization methods can be used similarly with the expressions in Sec. 2.

The fundamental principle of genetic optimization is to improve an initial random population towards an optimum in stages – generations – using evolutionary principles. To apply this algorithm to the situations considered here we define individuals and their fitness. A set of these individuals defines the population in each generation. Their fitness is a measure of optimality computed using the solution determined by the MoM solver.

Each individual corresponds to a single solution (combination of discrete mesh elements). Imposing a rule of numbering the elements of the mesh, the genotype of each individual is made of $N_x N_y$ possible genes in a single chromosome. Each gene determines if an element is metal or not present in a certain individual. A reasonable encoding for the genetic information is binary, 1 defining a metallic and 0 a non present element. At least two genes are eliminated from the genotype as the edge between them defines the feed of the antenna represented by the individual. Patterned antennas can also be optimized by removing some of the genes corresponding to the fixed metallic areas. An example of such patterned antennas is described in Sec. 3.2 and 5.3.

The fitness of the individuals is given by the optimized parameter/parameters. Usually a linear combination of parameters is evaluated for each individual. Such parameters may be the Q factor, matching, directivity, radiation pattern, metallic area, etc. These antenna parameters are computed here by an MoM solver with rectangular basis functions. Such basis functions usually decrease the number of MoM unknowns thus improving the solution time. Furthermore uniform discretization in both directions makes the basis functions equal (except for a spatial displacement).

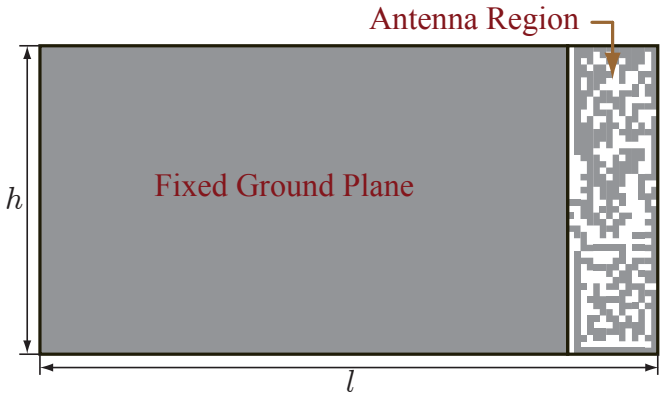

Figure 2: Example of simplified phone model with antenna region occupying approximately 15 % of the total length of the device.

This fact is exploited to further improve the solution time.

The integration of the electromagnetic solver into the optimization algorithm follows the description in [21, Ch. 9]. The mother impedance matrix (2.7) of size $N = 2N_xN_y - N_x - N_y$ is computed once prior to the optimization. During the optimization the genotype of each individual determines which rows and columns of (2.7) compile the impedance matrix describing that individual. The rows and columns with the same indexes compile the matrices corresponding to $\mathbf{X}_\mathrm{e}$, $\mathbf{X}_\mathrm{m}$ and $\mathbf{R}_\mathrm{rad}$ for each individual. The impedance matrix is used to compute the surface current density. This current can be used to compute other relevant parameters, *e.g.*, Q factor (2.12), radiation pattern, radiation resistance, etc. The advantage of this approach is that impedance matrix compilation time is smaller than computation time with formulation (2.7).

3.2 Antennas Integrated into Devices

From the electromagnetic wave generation point of view, many mobile devices that integrate antennas can be thought of as consisting of two spatial domains. One of the domains is represented by the space reserved for the structure (antenna) fed by the transmitter(s). This domain will be denoted in the following as the antenna region. The other domain contains all other parts integrated in the device. This domain usually contains metallic parts that act as ground for the structure in the antenna region. For this reason the second domain will be denoted ground plane in the following. In general the structures in both domains contribute to the radiated fields. It is also observed that the antenna region usually occupies a small fraction of the entire device.

We consider planar rectangular structures to further simplify the description of the previous paragraph. The two domains introduced above are defined as in Fig. 2. The optimization algorithm searches for metallic structures that may take arbitrary shapes within the antenna region. The other domain is a fixed rectangular metallic

ground plane. This ground plane extends a significant part of the structure (75, 85 and 94 % of the area for the structures in Sec. 5.3). The metal is considered lossless as in the previous section, *i.e.*, PEC. Such structures can be studied using the same approach as in Sec. 3.1. However this implementation is rather inefficient due to the presence of the fixed ground plane. The large extent of this ground plane in the structure translates into large individual impedance matrices (*i.e.*, comparable in size with the mother impedance matrix). Such large matrices may result in an MoM solution time prohibitive for optimization.

It is more computationally efficient to use block matrix decomposition as described in [16, 21]. The solution of the MoM algorithm can be obtained from the system of equations

$$\begin{pmatrix} \mathbf{Z}_{\mathrm{AA}} & \mathbf{Z}_{\mathrm{AG}} \\ \mathbf{Z}_{\mathrm{GA}} & \mathbf{Z}_{\mathrm{GG}} \end{pmatrix} \begin{pmatrix} \mathbf{J}_{\mathrm{A}} \\ \mathbf{J}_{\mathrm{G}} \end{pmatrix} = \begin{pmatrix} \mathbf{V} \\ \mathbf{0} \end{pmatrix} \tag{3.1}$$

where the indexes A and G denote the antenna region and the ground plane respectively, $\mathbf{Z}_{\mathrm{AA}}$, $\mathbf{Z}_{\mathrm{AG}}$, $\mathbf{Z}_{\mathrm{GA}}$ and $\mathbf{Z}_{\mathrm{GG}}$ denote blocks of elements of the mother impedance matrix (2.7) with pq correspondingly in the domains defined by AA, AG, GA, GG, $\mathbf{J}_{\mathrm{A}}$ and $\mathbf{J}_{\mathrm{G}}$ are the blocks of basis function coefficients that define the current flowing on the antenna region and ground plane respectively, and $\mathbf{V}$ is the matrix corresponding to the feeding model. The structure is fed only in the antenna region, thus the $\mathbf{0}$ in the right hand side. The solution is

$$\begin{cases} \mathbf{J}_{\mathrm{A}} &= (\mathbf{Z}_{\mathrm{AA}} - \mathbf{Z}_{\mathrm{AG}}\mathbf{Z}_{\mathrm{GG}}^{-1}\mathbf{Z}_{\mathrm{GA}})^{-1}\mathbf{V} \\ \mathbf{J}_{\mathrm{G}} &= -\mathbf{Z}_{\mathrm{GG}}^{-1}\mathbf{Z}_{\mathrm{GA}}\mathbf{J}_{\mathrm{A}} = \mathbf{Z}'\mathbf{J}_{\mathrm{A}} \end{cases} \tag{3.2}$$

The preprocessing becomes more computationally demanding due to the necessity to express the inverse of $\mathbf{Z}_{\mathrm{GG}}$. However this does not affect the actual optimization process because the size of the matrices manipulated during this process reduces to the size of $\mathbf{Z}_{\mathrm{AA}}$ using a concept similar to the mother impedance matrix for the right hand sides of (3.2). Using the same approach the evaluation of the stored energies and radiated power necessary for the evaluation of the Q factor (2.12) can be improved:

$$\mathbf{J}^{\mathrm{H}}\mathbf{X}_{\mathrm{e}}\mathbf{J} = \mathbf{J}_{\mathrm{A}}^{\mathrm{H}}\left(\mathbf{X}_{\mathrm{e,AA}} + 2\,\mathrm{Re}\{\mathbf{X}_{\mathrm{e,AG}}\mathbf{Z}'\} + \mathbf{Z}'^{\mathrm{H}}\mathbf{X}_{\mathrm{e,GG}}\mathbf{Z}'\right)\mathbf{J}_{\mathrm{A}} \tag{3.3}$$

where $\mathbf{X}_{\mathrm{e,AA}}$, $\mathbf{X}_{\mathrm{e,AG}}$ and $\mathbf{X}_{\mathrm{e,GG}}$ are the blocks of $\mathbf{X}_{\mathrm{e}}$ defined in the same way as those of $\mathbf{Z}$. It should be noted that the block matrix decomposition is performed in terms of basis functions, *i.e.*, the matrix elements in (3.1) correspond to basis functions defined on adjacent mesh elements. The inherent overlapping of the basis function domains of definition allows the existence of metallic elements supporting basis functions across the border between the ground plane and antenna region.

4 Physical Bounds

Physical bounds may be used as stopping criterion for an optimization process. They can also be used to compare the performance of optimized antennas. This

comparison is illustrated in Sec. 5.2 and 5.3 respectively for antennas limited to rectangular regions and antennas with a fixed rectangular ground plane. These antennas are obtained through a genetic optimization process stopped by genetic stability during 50 generations. The Q factors of these antennas do not deviate more than 30 % from their physical bound. This suggests that carefully integrated bounds may be used as stopping criterion in optimization algorithms.

The results in [6, 9] are used to derive the physical bounds for antennas whose shapes are limited to rectangular regions[2]. The maximum D/Q ratio is computed with closed form expressions assuming main radiation direction orthogonal to the rectangle. The physical bound for the Q factor can be derived further assuming that the antenna has directivity 1.5. The previous assumptions hold for many electrically small antennas.

Bounds for antennas with a fixed rectangular ground plane, see Fig. 2, are computed using the procedure described in [8, 10]. This procedure can be applied to structures with arbitrary shapes. The problem of determining the physical bound for the D/Q quotient of an antenna is solved using convex optimization [8]. This problem is equivalent to minimizing the energy stored in the fields excited by the antenna [10]. The current that minimizes this energy is determined by convex optimization. This current gives the minimum Q factor of an antenna and the maximum D/Q quotient achievable by that antenna. It should be noted that this current may be unphysical thus impossible to excite on real structures. In this formulation it is assumed that the main radiation direction is orthogonal to the structure.

The bounds [8, 10] become those in [6, 9] when the antenna region occupies the entire rectangular region, *i.e.*, when antennas limited by a rectangular region are solved by convex optimization.

5 Results

5.1 Simulation Setup

The genetic algorithm used here is based on Holter's implementation distributed with the PB-FDTD package [23]. We use a 200 individual population. Using tournament selection 80 randomly chosen individuals compete to become one of two breeding parents. Child generation is subjected to crossover and mutation. Offspring are generated in pairs and returned to the initial population. Then the population is decreased by removing the least fit two individuals.

Crossover happens at two random positions in the genotype with probability 0.8. The mutation rate is 0.2 when the population evolves naturally; in this situation a single gene is mutated at a time. The probability of mutation becomes 1 when the population does not improve during an entire generation. In all succeeding generations, all offspring will have 10 random genes mutated at a time. Due to randomness, the actual number of genes that are mutated may take any value between 1 and 10. If a new individual with better performance is found, the evolution returns

[2] see also http://www.mathworks.com/matlabcentral/fileexchange/26806-antennaq

to "natural" conditions, 0.2 single gene mutation probability. This behavior should increase the chances of finding better solutions in less generations. Even though the population evolution shows the expected behavior, a thorough performance study has not been carried out.

The stop condition of the algorithm is genetic stability of the population during 50 generations. This condition can be replaced by the best individual performance in the current population. When this performance is close enough to the physical bounds [6, 8–10] the optimization process can be stopped.

The objective function of the optimization algorithm is a linear combination of antenna parameters, *i.e.*,

$$\text{minimize} \qquad \alpha_{\mathrm{Q}} Q + \alpha_{\mathrm{R}} \left| \frac{\mathbf{J}^{\mathrm{H}} \mathbf{X}_{\mathrm{e}} \mathbf{J} - \mathbf{J}^{\mathrm{H}} \mathbf{X}_{\mathrm{m}} \mathbf{J}}{\mathbf{J}^{\mathrm{H}} \mathbf{R}_{\mathrm{rad}} \mathbf{J}} \right| + \alpha_{\mathrm{A_N}} A_{\mathrm{N}}, \tag{5.1}$$

where α_{Q}, α_{R} and $\alpha_{\mathrm{A_N}}$ are the weights associated with the Q factor, resonance and normalized metallic area A_{N}, respectively. For illustrative purpose resonance is evaluated from the difference between the stored electric and magnetic energies. This difference is normalized to the radiated power. The area is normalized to the entire rectangular region area (antenna region area for antennas with a rectangular ground plane).

The weights introduced in the previous paragraph control the optimization process. Either α_{Q} or α_{R} is emphasized at a time for obtaining the data presented in the following. As a result either antennas with minimum Q or resonant are targeted, respectively. The normalized area weight has been maintained constant, $\alpha_{\mathrm{A_N}} = 1$. This parameter has been included in order to decrease the metallic area of the structures and eliminate some isolated mesh elements.

The MoM solver integrated into the genetic algorithm is an EFIE based in-house simulator. Galerkin testing is used [19] with rooftop basis and testing functions. The amplitudes of these functions have linear variation on two adjacent mesh elements, as exemplified in Fig. 1. Their direction is perpendicular to the common edge and pointing from the first to the second mesh element (considering a numbering rule imposed on the elements).

The optimization results are compared with simulation data obtained from the Efield MoM solver. This solver uses rooftop basis functions defined on triangular mesh elements. Non-self-resonant antennas have been loaded inductively such that they achieve resonance at the frequency they were optimized for. This loading has been used to confirm that tuning does not change the performance of the optimized antennas.

5.2 Rectangular Regions

The optimization algorithm has been run for rectangular regions with an aspect ratio of $l/h = 2$. Such regions can achieve the maximum D/Q ratio when operated optimally, [9, 10]. The antennas inside these regions are considered thin metallic sheets without losses, *i.e.*, PEC. The frequencies were chosen such that the electrical dimensions are in the range $kl = 0.1 \ldots 1.3$ ($ka \approx 0.06 \ldots 0.7$). In this way

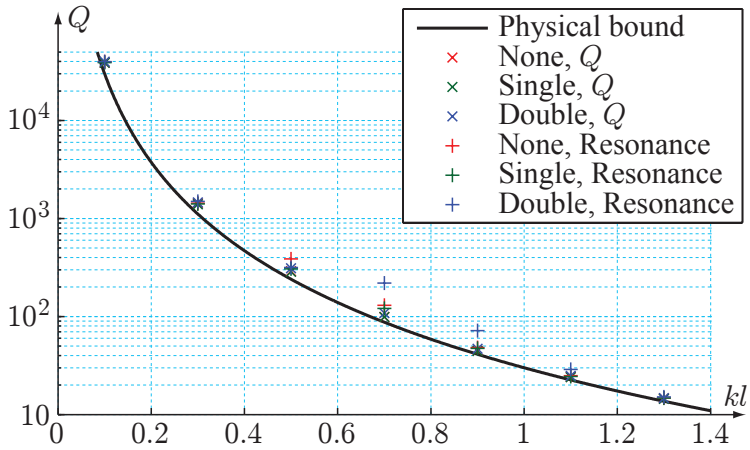

Figure 3: Optimized antenna Q factors compared with the physical bound [6, 9, 10] for rectangular regions. The best result from 5 runs for each symmetry (none, single and double) and optimization criterion (Q factor or resonance) is depicted.

some of the electrical dimensions usually considered small have been studied. The discretization was $N_x = 64$, $N_y = 32$ such that the discrete elements are square. A voltage gap model has been used to feed the antennas. Two mesh elements have been marked as fixed metallic areas and removed from the genotype. These elements are the two closest to the center of the rectangular region such that the voltage drop is applied along the x-direction, see Fig. 1.

From the symmetry point of view, three groups of structures have been considered: non-symmetric, symmetric with respect to $\hat{\boldsymbol{x}}$ and symmetric with respect to $\hat{\boldsymbol{x}}$ and $\hat{\boldsymbol{y}}$, see Fig. 1. These are denoted as "None", "Single", and respectively "Double" in Figs 3 and 4. The corresponding number of genes in the genotype is: 2046, 1023 and 512.

Two optimization criteria have been imposed. They target to find either antennas with the optimal Q or antennas as close as possible to a resonance. The corresponding objective functions have $\alpha_{\mathrm{Q}} = 4$, $\alpha_{\mathrm{R}} = 1$ and $\alpha_{\mathrm{Q}} = 1$, $\alpha_{\mathrm{R}} = 4$ respectively.

The smallest Q factor of 5 optimized antennas for each symmetry and criterion is depicted in Fig. 3. The physical bound for a rectangular region with the same dimensions is computed using the results in [6, 9, 10] and included for comparison. This computation is performed assuming main radiation direction orthogonal to the rectangle and directivity 1.5. The relative deviation of the Q factor from this physical bound is depicted in Fig. 4. The antennas with the smallest Q in all runs per kl value have been simulated with Efield. Four of these antennas are depicted in Fig. 5. The resulting Q factors computed according to [7, 26] are included in Fig. 4 for comparison. These antennas have radiation patterns resembling that of an electric dipole. Their directivities are between 1.49 and 1.52 in a direction within 30° of the normal of the rectangle.

Some observations can be made even though the number of runs is rather small.

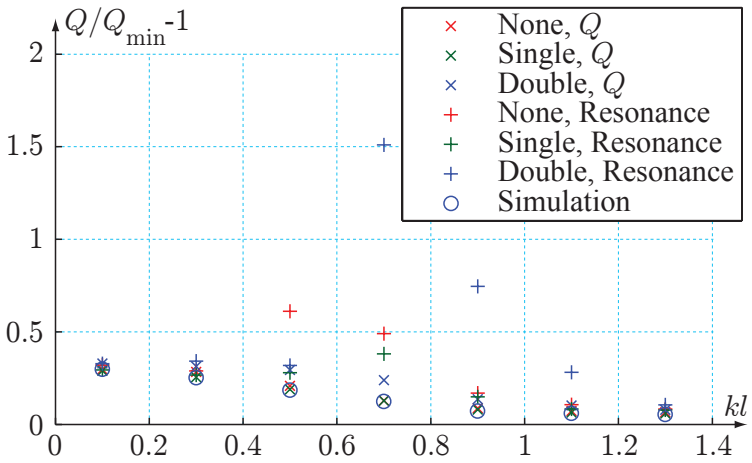

Figure 4: Deviation of the Q factors depicted in Fig. 3 relative to the physical bound Q_{min} [6, 9, 10]. The deviations of the Q factors computed from simulation data using the procedure in [7, 26] are also included.

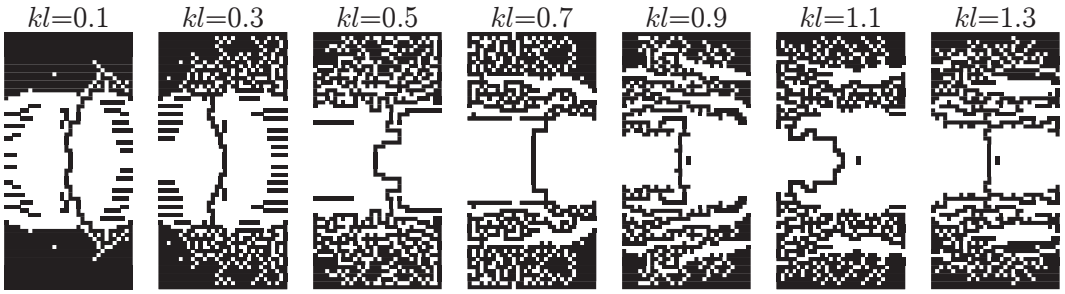

Figure 5: Four of the structures simulated in Efield whose Q factors are depicted in Fig. 3. Feeding edges are circled.

Antennas symmetric in the l-direction have the smallest Q factors. Antennas symmetric in both l and h-directions have the greatest Q factors. Intermediate Q factors are obtained by antennas that are non-symmetric. The genetic algorithm can find antennas which perform within 10% of the physical bound when their dimensions are somewhat larger. When the antenna dimensions are smaller, the optimizer finds antennas about 30% away from the physical bound. Antennas optimized for resonance have a greater Q than those optimized for Q factor, significantly greater for some electrical dimensions. This happens partly due to the compromise made during the optimization in the disadvantage of the Q factor. This compromise modifies the genetic path followed by the antenna population based on the values involved in the computation of fitness with (5.1). However, a detailed study of the genetic path has not been carried out.

The optimized antennas show common characteristics that depend on their electrical size. A few such characteristics are given as examples in the following considering Fig. 5. The structure with $kl = 0.1$ has: large metallic regions at the extremities in the l-direction, little meandering that increases the longest current path, and metallic strips parallel to the h direction which grow in length towards the extremities of the structure. The structure with $kl = 0.5$ is heavily meandered with many short metallic stubs along the meander; it has less metallic h-aligned strips. Larger structures are dominated by shorter meandering path and longer stubs. A statistic study has not been carried out to establish the distribution of these characteristics among the optimized antennas.

5.3 Simple Phone Model

A simplified model of a mobile telephone as a radiating device is obtained by considering the device mostly metallic. In a limited region a specially devised metallic structure is fed by the transmitter. For further simplification the metal is considered lossless, *i.e.*, PEC, and the entire structure planar, see Fig. 2. It has been observed that an aspect ratio $l/h = 2$ describes many mobile devices in use today. The frequencies have been chosen such that the electrical dimensions are in the range $l/\lambda = 0.1 \ldots 0.5$. These frequencies are between 300 MHz and 1.5 GHz for an $l = 10$ cm device. The discretization was $N_x = 96$ and $N_y = 48$ for the entire structure (antenna region and ground plane). Such structures but with coarser rectangular element mesh are preliminarily investigated in [2]. The procedure presented in Sec. 3.2 has been applied to increase the speed of the optimization process. The structures are fed by a voltage gap such that their far field is mainly linearly polarized along the l dimension.

For illustration purpose the optimization procedure has been applied to two situations. In the first situation different dimensions of the antenna region have been imposed. The results of antenna optimization for minimum Q are presented in Fig. 6. The second situation illustrates the method for different optimization criteria and feeding positions, Fig. 7. Examples of optimized antenna regions obtained in the above mentioned situations are depicted in Fig. 8.

Three cases have been considered for the results in Fig. 6 where approximately

6 %, 15 % and 25 % of the structure length is occupied by the antenna region. The optimization procedure has been run five times for each set of electrical and antenna region dimensions considered. The optimization target was antennas with minimum Q ($\alpha_{\mathrm{Q}} = 10$, $\alpha_{\mathrm{R}} = 1$). The smallest Q obtained in the five runs is labeled "Prediction." The antennas having these smallest Q factors have been simulated in Efield. Their input impedance is differentiated following the procedure in [7, 26] to obtain the Q factors labeled "Simulation." These antennas have a main radiation direction within 30° of the normal of the rectangular region. The physical bounds [8] corresponding to radiating structures with a rectangular ground plane, normal main radiation direction and antenna regions occupying 6 %, 15 % and 25 % of the antenna length are included in Fig. 6. In addition the physical bound [6, 9, 10] of rectangular radiating structures with normal main radiation direction and directivity 1.5 is depicted in solid line.

It is observed in Fig. 6 that both the predicted and the simulated Q values follow closely the physical bounds for small electrical dimensions. The relative deviation of these values from the corresponding physical bound is smaller than 20 % in these cases. The deviation is greater for smaller antenna regions. When the electrical sizes of the structures increase, the values resulted from the simulation data deviate from the predicted values. The simulation values are smaller than the predicted values and bound. This happens due to the Q factor estimation procedure from the input impedance. Small Q values are estimated less accurately when multiple closely spaced resonances are present around the frequency of interest. The single resonance model [7, 26] was used to compute the Q for the structures with $l/\lambda = 0.1, 0.175$ and 0.25. The multiple resonance Brune synthesis model [25] was used to compute the Q for the structures with $l/\lambda = 0.325, 0.4$ and 0.475.

Four cases have been considered for the results in Fig. 7. They are defined by all the combinations of two feeding positions and two optimization targets applied to structures with the antenna region 15 % of the structure length. The two feeding positions are at the interface between the ground plane and the antenna region in the center of the h dimension and at the side of the structure. As optimization targets Q factor ($\alpha_{\mathrm{Q}} = 10$, $\alpha_{\mathrm{R}} = 1$) and resonance ($\alpha_{\mathrm{Q}} = 1$, $\alpha_{\mathrm{R}} = 10$) have been considered. The optimization algorithm has been run five times for each case and frequency. The relative deviations of the smallest Q factors obtained in the five runs are labeled "Prediction" in the figure. The reference for these relative deviations is the physical bound [8] for antenna regions occupying 15 % and normal main radiation direction. The antennas with these smallest Q factors have been simulated in Efield. Their input impedance gives the Q factors labeled "Simulation" using a resonance model [7, 25, 26]. These antennas have a main radiation direction within 30° of the normal of the structure. The observations pertaining to Figs 4 and 6 are also valid for Fig. 7.

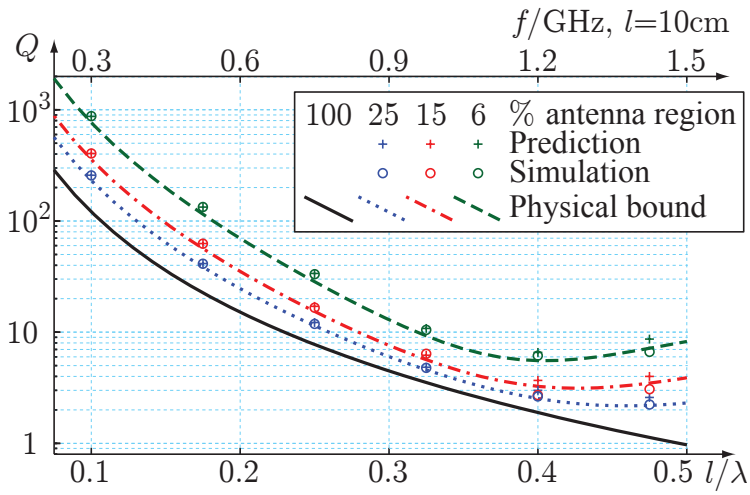

Figure 6: Optimized antenna Q factors compared with the physical bound. The smallest Q factor of five optimization algorithm runs per frequency and antenna region size is labeled "Prediction". The Q factors computed using the results in [7, 25, 26] from simulation data for the smallest Q antennas are labeled "Simulation". The physical bounds for radiating structures with rectangular ground planes [8] and antenna regions occupying 6, 15 and 25 % of antenna length (see Fig. 2) are depicted in dashed, dash-dot and dotted line, respectively. The physical bound for antennas limited to rectangular regions [6, 9, 10] is depicted in solid line.

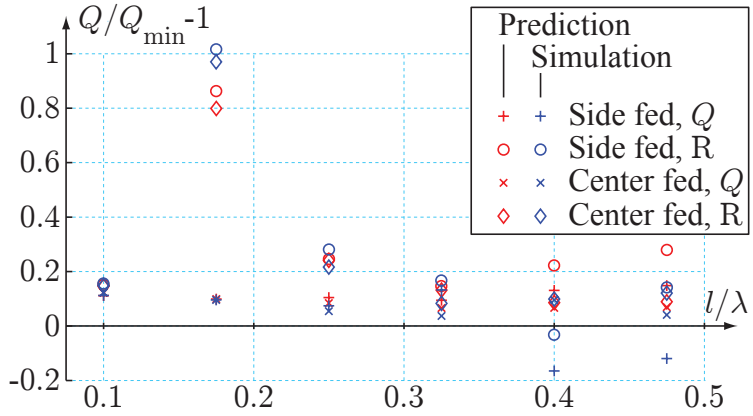

Figure 7: Deviation of optimized antenna Q factors relative to the physical bound [8] for 15 % antenna regions (see Fig. 2). The smallest Q factor from five optimization algorithm runs is labeled "Prediction". The Q factors computed using the results in [7, 25, 26] from simulation data for the smallest Q antennas are labeled "Simulation". Side and center feeding has been considered for structures optimized for Q factor and resonance (R).

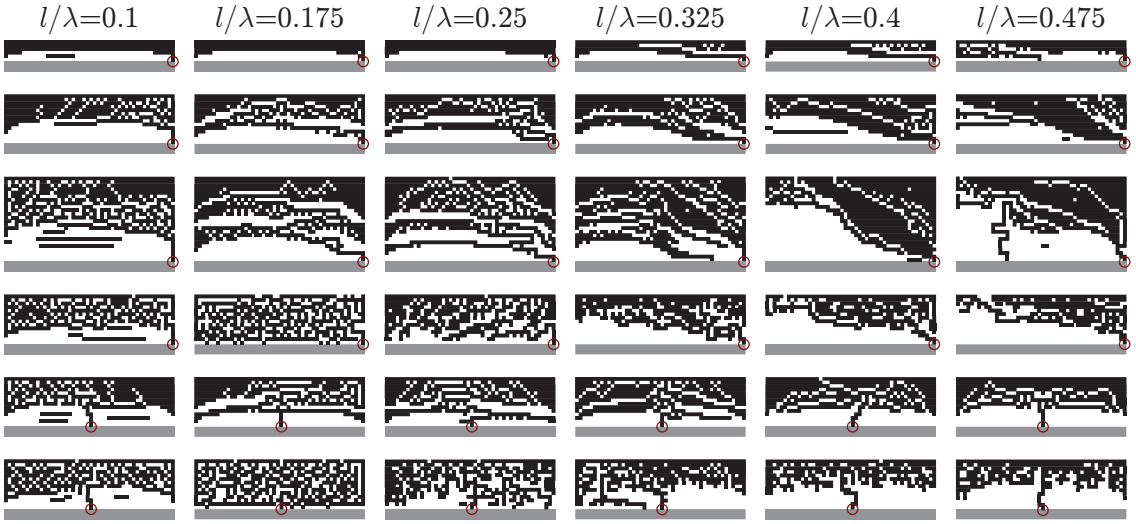

Figure 8: Example of antenna regions of structures simulated in Efield. Shaded – part of the ground plane. First three rows from top to bottom: side fed antenna regions occupying 6 %, 15 %, 25 % of antenna length optimized for Q factor. Row 4: side fed 15 % antenna regions optimized for resonance. Rows 5 and 6: center fed 15 % antenna regions optimized for Q factor and resonance, respectively. Feeding edges are circled.

6 Conclusions

A method of computing Q factors of radiating structures from single frequency simulation data is presented. This computation is based on the electric and magnetic energies stored in the fields excited by an antenna [24] evaluated following the procedure described in [8, 10]. Using this method it is possible to estimate antenna bandwidth from the current excited on the structure at a single frequency. This method has been applied to rectangular structures and structures with a rectangular ground plane describing in a simplified manner some mobile devices in use today. The resulting antennas perform close to the physical bounds in terms of their Q factors for many electrically small dimensions. Simulation data obtained from the commercial electromagnetic solver Efield agree very well with the theoretical results.

The method can be integrated very easily in a standard MoM solver. The temporal overhead added by such an integration is small due to the fact that most of the quantities needed are computed in standard MoM solvers. Thus using this method may reduce optimization time for some radiating structures. In addition it is possible to directly compare realized performance of optimized structures with their physical bounds [8]. The results presented confirm the validity of these physical bounds. Sub-optimum solutions resulted from optimization have "genetic" characteristics that may prove useful for the manual design of other radiating structures.

The results obtained using this method have been presented in terms of antenna Q factors. Other important antenna parameters such as radiation resistance,

matching and losses are the object of future work. More realistic structures will be considered there.

Acknowledgment

The support of the Swedish Research Council is gratefully acknowledged.

References

[1] Antenna Standards Committee of the IEEE Antennas and Propagation Society. IEEE Standard Definitions of Terms for Antennas, 1993. IEEE Std 145-1993.

[2] M. Cismasu and M. Gustafsson. Illustration of mobile terminal antenna optimization by genetic algorithms with single frequency simulation. In *Electromagnetic Theory (EMTS), Proceedings of 2013 URSI International Symposium on*, pages 84–87, 2013.

[3] R. Fletcher. *Practical Methods of Optimization.* John Wiley & Sons, Ltd., Chichester, 1987.

[4] W. Geyi. A method for the evaluation of small antenna Q. *IEEE Trans. Antennas Propagat.*, **51**(8), 2124–2129, 2003.

[5] P. E. Gill, W. Murray, and M. H. Wright. *Practical Optimization.* Academic Press, London, 1981.

[6] M. Gustafsson, M. Cismasu, and S. Nordebo. Absorption efficiency and physical bounds on antennas. *International Journal of Antennas and Propagation*, **2010**(Article ID 946746), 1–7, 2010.

[7] M. Gustafsson and S. Nordebo. Bandwidth, Q-factor, and resonance models of antennas. *Progress in Electromagnetics Research*, **62**, 1–20, 2006.

[8] M. Gustafsson and S. Nordebo. Optimal antenna currents for Q, superdirectivity, and radiation patterns using convex optimization. *IEEE Trans. Antennas Propagat.*, **61**(3), 1109–1118, 2013.

[9] M. Gustafsson, C. Sohl, and G. Kristensson. Illustrations of new physical bounds on linearly polarized antennas. *IEEE Trans. Antennas Propagat.*, **57**(5), 1319–1327, May 2009.

[10] M. Gustafsson, M. Cismasu, and B. L. G. Jonsson. Physical bounds and optimal currents on antennas. *IEEE Trans. Antennas Propagat.*, **60**(6), 2672–2681, 2012.

[11] M. Gustafsson and B. Jonsson. Stored electromagnetic energy and antenna Q. Technical Report LUTEDX/(TEAT-7222)/1–25/(2012), Lund University, Department of Electrical and Information Technology, P.O. Box 118, S-221 00 Lund, Sweden, 2012. http://www.eit.lth.se.

[12] R. F. Harrington. *Field Computation by Moment Methods.* Macmillan, New York, 1968.

[13] R. L. Haupt and D. H. Werner. *Genetic Algorithms in Electromagnetics.* Wiley-IEEE Press, 2007.

[14] R. W. Jackson and D. M. Pozar. Full-wave analysis of microstrip open-end and gap discontinuities. *IEEE Trans. Microwave Theory Tech.*, **33**(10), 1036–1042, 1985.

[15] J. M. Jin. *Theory and Computation of Electromagnetic Fields.* Wiley, 2011.

[16] J. M. Johnson and Y. Rahmat-Samii. Genetic algorithms and method of moments GA/MOM for the design of integrated antennas. *IEEE Trans. Antennas Propagat.*, **47**(10), 1606–1614, oct 1999.

[17] L. S. Lasdon. *Optimization Theory for Large Systems.* Dover Books on Mathematics. Dover Publications, 2002.

[18] J. R. Mosig and F. E. Gardiol. A dynamical radiation model for microstrip structures. In P. W. Hawkes, editor, *Advances in Electronics and Electron Physics*, volume 59, pages 139 – 237. Academic Press, 1982.

[19] A. F. Peterson, S. L. Ray, and R. Mittra. *Computational Methods for Electromagnetics.* IEEE Press, New York, 1998.

[20] D. M. Pozar. Considerations for millimeter wave printed antennas. *IEEE Trans. Antennas Propagat.*, **31**(5), 740–747, September 1983.

[21] Y. Rahmat-Samii and E. Michielssen. *Electromagnetic Optimization by Genetic Algorithms.* Wiley Series in Microwave and Optical Engineering. John Wiley & Sons, 1999.

[22] J. Robinson and Y. Rahmat-Samii. Particle swarm optimization in electromagnetics. *IEEE Trans. Antennas Propagat.*, **52**(2), 397 – 407, feb. 2004.

[23] B. Thors, H. Steyskal, and H. Holter. Broad-band fragmented aperture phased array element design using genetic algorithms. *IEEE Trans. Antennas Propagat.*, **53**(10), 3280 – 3287, oct. 2005.

[24] G. A. E. Vandenbosch. Reactive energies, impedance, and Q factor of radiating structures. *IEEE Trans. Antennas Propagat.*, **58**(4), 1112–1127, 2010.

[25] O. Wing. *Classical Circuit Theory.* Springer, New York, 2008.

[26] A. D. Yaghjian and S. R. Best. Impedance, bandwidth, and Q of antennas. *IEEE Trans. Antennas Propagat.*, **53**(4), 1298–1324, 2005.